Volume 1 | Number 1 | Jan 2013 | Pages 1–100

Journal of
Materials Chemistry A

Materials for energy and sustainability
www.rsc.org/materialsA

ROYAL SOCIETY
OF CHEMISTRY

ROYAL SOCIETY
OF CHEMISTRY

www.rsc.org/materialsA

Journal of Materials Chemistry A

Dynamic Article Links ▶

COMMUNICATION

Highly Efficient and Stable Organic Sensitizers with Duplex Starburst Triphenylamine and Carbazole Donors for Liquid and Quasi-solid-state Dye-sensitized Solar Cells

Li-Lin Tan,[a] Jian-Feng Huang,[a] Yong Shen,[a] Li-Min Xiao,[b] Jun-Min Liu,*[a] Dai-Bin Kuang,[a] and Cheng-Yong Su*[ac]

Two new D-D-π-π-A type stable organic sensitizers DT3 and DW3 were successfully synthesized for dye-sensitized solar cells. DT3 displayed η values of 10.03% and 8.05% in liquid and quasi-solid-state DSSCs, respectively, under standard global 1.5 solar conditions, offering an example achieving the highest efficiency to date in quasi-solid-state DSSCs based on pure organic dye.

Dye-sensitized solar cells (DSSCs) as green energy have been intensively studied to improve the sensitizer which plays crucial role to determine the power conversion efficiency (η) as well as cell stability.[1] To date, overall conversion efficiencies of up to 12%,[2] 11%[3] and 10%[4] were achieved from liquid DSSCs by employing zinc, ruthenium complex and pure organic dyes, respectively, but the devices are subject to long-term instability. Quasi-solid-state (QSS) DSSCs have been supposed as potential candidates to overcome this problem and improve commercial development.

Compared to metal complex dyes which are usually expensive and hard to purify, the pure organic dyes, commonly constructed into a donor-π bridge-acceptor (D-π-A) configuration, feature in high extinction coefficient and low cost. However, up to now, their open circuit voltage (V_{oc}) and long-term stability still fall behind metal complex dyes.[5] One main reason for lower V_{oc} of the organic dyes is due to the strong interaction between iodine and organic dye and, leading to the fast recombinaton of electrons. In order to solve the problem, one strategy is to introduce more donor units to the primary donor, thereby forming cone-shaped D-D-π-A structures. In contrast to normal rod-shaped analogues,[6] cone-shaped dyes are beneficial for better thermostability and lower aggregation tendency. Besides, their absorption regions can be broadened and molar extinction coefficients be increased. Several groups have accomplished such strategy by transforming the rod-shaped dye into a starburst type, usually employing triarylamine units as the donor, to improve the V_{oc} value. This enhancement should be attributed to their aggregation-resistant nonplanar configuration and multiphenyl segments on the starburst triarylamine, which can block the approach of triiodide in the electrolyte.[5a,7] On the other hand, the

poor stability of organic dyes in DSSCs is mainly ascribed to the formation of excited triplet states and unstable radicals. An efficient approach to tackle this problem is to incorporate an oligothiophene moiety into the organic framework, where the radical center could be delocalized among the dye cation.[8]

Along this line, we recently reported a starburst D-D-π-A organic sensitizers (**D3**) using triarylamine (TPA) and carbazole as duplex electron donors, 3,4-ethoxythiophene (EDOT) unit as π-spacer, and cyanoacetic acid as electron acceptor, yielding 6.15% power conversion efficiency under AM 1.5 G irradiation.[9] Herein we improved the structural model and synthesized two new starburst sensitizers **DT3** and **DW3**, which form D-D-π-π-A type organic dyes by incorporating 3,4'-dihexyl-2,2'-bithiophene besides EDOT moiety to act as the duplex π-spacers (Scheme 1). The optical, electronic and photovoltaic studies unveiled outstanding η values for **DT3** in both liquid DSSCs (10.03%) and quasi-solid-state (QSS) DSSCs (8.05%) under AM 1.5 G irradiation. To the best of our knowledge, the former is comparable with the hitherto world record of organic dye in liquid DSSCs while the latter represents the highest efficiency so far observed for QSS-DSSCs based on pure organic sensitizers.[4,7a,10]

This journal is © The Royal Society of Chemistry [year]

J. Mater. Chem. A, 2014, **[vol]**, 00–00 | 1
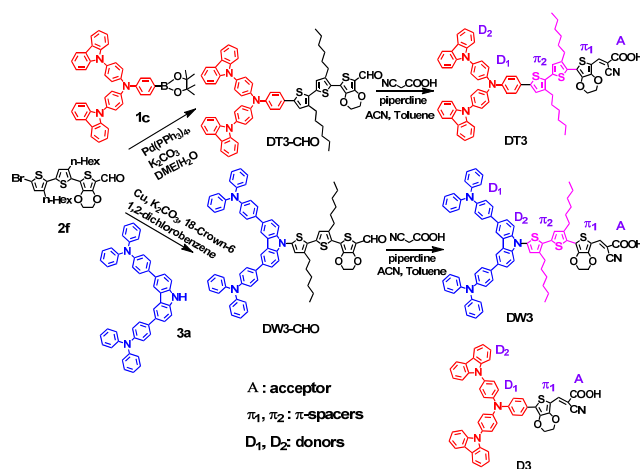
Scheme 1 Synthetic route for **DT3** and **DW3** in comparison with known **D3**.

The synthetic route of **DT3** and **DW3** is outlined in Scheme 1. **DT3-CHO** was synthesized by Suzuki coupling reaction of **1c** and **2f** in the presence of KCO_3 as base and $Pd(PPh_3)_4$ as catalyst. **DT3** was obtained by Knoevenagel condensation with cyanoacetic acid, which can convert carbaldehydes to cyanoacrylic acids. The dye **DW3** was conveniently synthesized from **3a** and **2f** via a two-step process involving phase transfer catalyzed N-alkylation, followed by Knoevenagel condensation of aldehydes with cyanoacetic acid.

The UV-vis absorption spectra of **DT3** and **DW3** in $CHCl_3$ are shown in Fig. 1. The spectrum of **DT3** exhibits two maxima at 512 nm (32800 M^{-1} cm^{-1}) and 341 nm (36500 M^{-1} cm^{-1}, showing a shoulder at 380 nm). The former is attributed to intramolecular charge transfer (ICT) between the starburst donor and the cyanoacrylic acid while the later arises from the π-$\pi*$ electron transition. Under the same conditions, the **DW3** sensitizer displays absorption bands at 490 nm (30700 M^{-1} cm^{-1}) and 340 nm (64900 M^{-1} cm^{-1}). It is clear that the extinction coefficient of π-π^* transition in **DW3** is higher than **DT3**, apparently owing to the larger conjugated system in the electron donor unit. This is in accordance with the computation results that the oscillation strength of the second absorption band in **DW3** is stronger than **DT3** (Table S1). However, **DT3** exhibits enhanced molar extinction coefficient in the ICT band and the absorption bands red-shift to larger numbers, which are due to the stronger donor and better coplanarity between the electron donor and acceptor in **DT3**,[7b] as verified by the computation results. Upon adsorption of the dyes on TiO_2 films, the absorption bands are broadened and red-shift can be observed (Fig. S1), most likely due to electronic coupling of the dyes on TiO_2 surface.[7c]
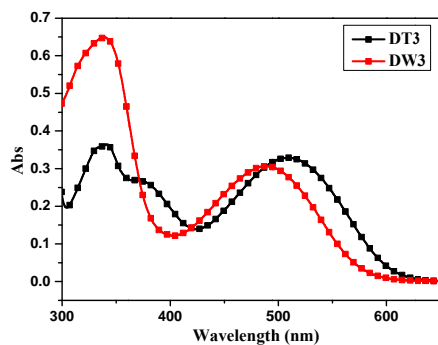

Fig. 1 The absorption spectra of **DT3** and **DW3** in $CHCl_3$ solution.

The moderately high oxidation potentials were found for **DT3** and **DW3** and the zero-zero excitation energy (E_{0-0}) was calculated from the absorption onset to estimate the excited state potential (E_{0-0}^*). The deduced E_{0-0}^* values (**DT3**, -1.0 and **DW3**, -0.80 V, versus NHE, normal hydrogen electrode) are more negative than the bottom of TiO_2 conduction band (-0.5 V vs NHE), indicating that the electron injection process is energetically permitted. On the other hand, the first oxidation potentials of the dyes (**DT3**, 1.12 and **DW3**, 1.39 V vs NHE) are more positive than the iodine/iodide redox potential value (~ 0.4 V vs NHE), thus allowing an effective dye regeneration and suppressing the recapture of injected electrons by the dye cation radical.

Molecular-orbital calculations (Fig. 2) indicate that the HOMO levels of **DT3** and **DW3** are delocalized mainly at the donor group consisting of TPA and carbazole, and further extend to the carbazole or TPA core. Examination of the molecular orbitals of both sensitizers illustrates that the HOMOs in **DT3** are more delocalized on the π bridge than **DW3**, because of its better coplanarity in conjugated pathway. The LUMOs of **DT3** and **DW3** are located in the cyanoacrylic moiety through dithiophene and EDOT. As a result, the HOMO-LUMO excitation could transfer the electron distribution from the starburst donor to cyanoacrylic acid moiety through the π-conjugation bridge.

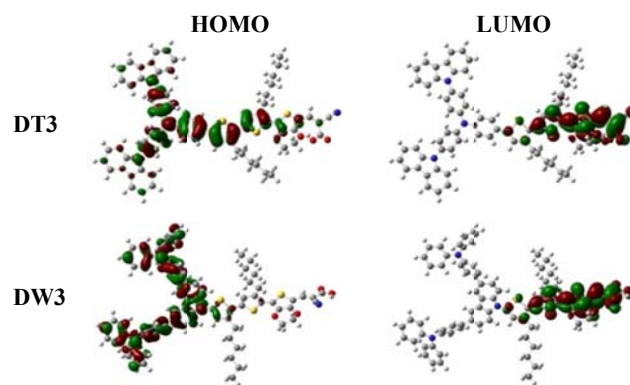HOMO   LUMO

Fig. 2 Frontier molecular orbitals (HOMO and LUMO) of **DT3** and **DW3** calculated with DFT on the B3LYP/6-31G* level.

The photovoltaic performance of **DT3**- and **DW3**-sensitized solar cells with liquid and quasi-solid-state electrolyte is shown in Fig. 3, and the detailed parameters with are listed in Table 1. The photocurrent action spectra of liquid DSSCs were obtained using an electrolyte comprising 0.6 M 1-methyl-3-propyl imidazolium iodide (PMII), 0.1 M guanidinium thiocyanate (GuNCS), 0.05 M LiI, 0.03 M I_2, 0.5 M tert-butylpyridine in a mixture of acetonitrile and valeronitrile (85:15, v/v). The incident-photon-to-current conversion efficiency (IPCE) of **DT3** exceeds 81% in the range of 410-610 nm, reaching the highest value of 91% at 481 nm. Under the same conditions, the IPCEs for **DW3** decrease above 500 nm toward the long-wavelength region. The results indicate stronger light harvesting ability for **DT3**. Under standard global AM 1.5 solar conditions, **DT3**-sensitized solar cells give a short circuit photocurrent density (J_{sc}) of 19.18 mA cm^{-2}, an open circuit voltage (V_{oc}) of 752 mV, and a fill factor (ff) of 0.70, corresponding to an overall η of 10.03%, which is amongst the highest reported values for DSSCs based on organic sensitizers.[4,7a] In contrast, the **DW3**-sensitized solar cells give a J_{sc} of 18.42 mA cm^{-2}, a V_{oc} of 745 mV, and an ff of 0.67, corresponding to a η of 9.15%. Since the π-conjugated bridge and electron acceptor of the two dyes are identical, the superior performance of **DT3** over **DW3** can be traced to the subtle modification in the structural design of the donor moieties (**D1** and **D2**).
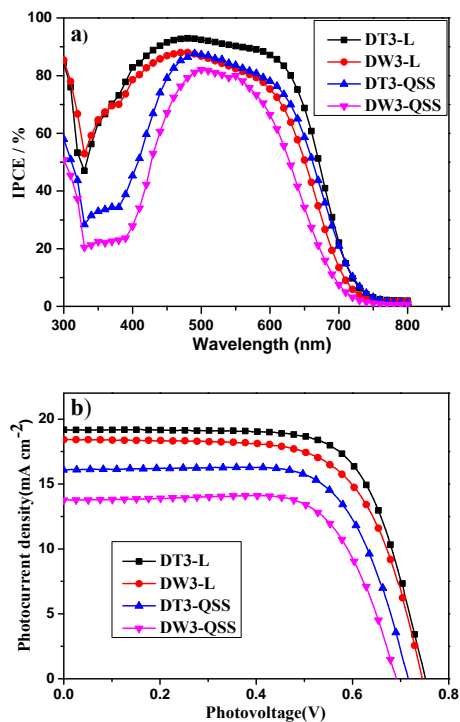
2 J. Mater. Chem. A, 2014, **[vol]**, 00–00

This journal is © The Royal Society of Chemistry [year]

Fig. 3 (a) Photocurrent action spectrum and (b) current-voltage characteristics of **DT3**- and **DW3**-sensitized solar cells with volatile and quasi-solid-state electrolyte (L: liquid DSSCs, QSS: quasi-solid-state DSSCs).

Table 1 Performance parameters of DT3 and DW3-sensitized solar cells with volatile and QSS electrolyte

dye	electrolyte	J_{sc}/mA cm^{-2}	V_{oc}/mV	FF	η(%)
DT3	liquid	19.18	752	0.70	10.03
DW3	liquid	18.42	745	0.67	9.15
N719	liquid	16.40	765	0.69	8.70
DT3	quasi-solid	16.08	716	0.70	8.05
DW3	quasi-solid	13.75	691	0.71	6.75
N719	quasi-solid	10.75	749	0.75	6.07

Electrochemical impedance spectroscopy (EIS) analyses were also carried out to clarify the above photovoltaic findings. A large semicircle in the Nyquist plot (Fig. 4) represents the charge recombination (R_r) at the interface of the TiO$_2$/electrolyte. A smaller R_r value indicates faster electron recombination from TiO$_2$ to electron acceptors in an electrolyte and thus resulting in lower V_{oc}. Therefore, the shorter semicircle radius of **DW3** indicates that its electron recombination resistance is smaller than **DT3**. Electron lifetime (τ) derived from curve fitting are 242.1 and 301.2 ms for **DW3** and **DT3**, respectively (Table S2), which agrees well with the trend of V_{oc} values. The increase in electron lifetime in the TiO$_2$ film is accompanied by a pronounced rise in the charge transfer resistance, which relies on the sensitizer structure as a result of different coverage of dyes on the TiO$_2$ surface. It is known that the sensitizer adsorption amount heavily

affect the lifetime and V_{oc}, and therefore, the shorter lifetime of starburst sensitizer **DW3** was probably attributed to its lower dye packing density on TiO$_2$ compared to **DT3** (adsorbed amounts of **DT3** and **DW3** are 2.2×10^{-7} and 1.7×10^{-7} mol cm^{-2}, respectively), which would result in higher I$_3^-$ concentration in the vicinity of TiO$_2$ surface and smaller charge recombination resistance.
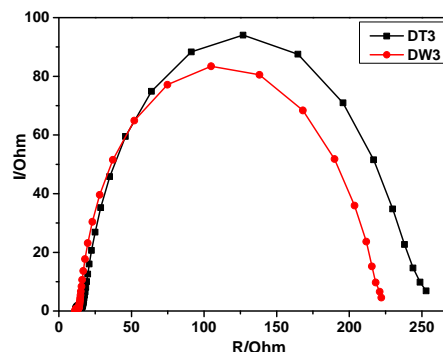

Fig. 4 EIS Nyquist plots (i.e. minus imaginary part of the impedance -Z '' vs the real part of the impedance Z' when sweeping the frequency) for **DT3**- and **DW3**-sensitized solar cells.

For QSS-DSSCs evaluation, silica nanoparticles were mixed with 0.5 M iodine and 0.45 M benzimidazole (BI) in pure 1-butyl-3-methylimidazolium iodide (BMII) to prepare ionic liquid-based QSS electrolyte. As seen in Fig. 3, the IPCE data exceed 70% for **DT3** and 50% for **DW3** in the spectral range of 435-630 nm, while the maxima of **DT3** and **DW3** reach 87% at 490 nm and 82% at 500 nm, respectively. The IPCE value of **DT3** in the range of 400 to 700 nm is higher than **DW3**, suggesting that **DT3** is more attractive because more extended absorption spectra will enhance cell efficiency. Under standard global AM 1.5 solar conditions, the QSS-DSSCs using **DT3** as sensitizer exhibit J_{sc} of 16.08 mA cm^{-2}, V_{oc} of 716 mV and ff of 0.70, while the overall η reaches 8.05%. This high η value represents the highest efficiency ever reported for QSS-DSSCs based on metal-free sensitizers,[7a,10] is also far superior than analogous QSS-DSSCs based on metal complex dye N719 (η = 6.07%). However, it should be noted that higher efficiencies have been observed for QSS-DSSCs based on ruthenium complex dye in polymer gel electrolytes,[11] implying that the present organic dye **DT3** may achieve even higher efficiency by using polymer gel electrolytes in QSS-DSSCs (investigation is under way in our group). Under the same conditions, QSS-DSSCs based on **DW3** give a J_{sc} value of 13.75 mA cm^{-2}, a V_{oc} of 691 mV, and an *ff* of 0.71, corresponding to the η value of 6.78%. **DT3** shows higher η than **DW3** in QSS-DSSCs, which might be attributed to its wider IPCE spectra, better dye adsorption on TiO$_2$, and higher injection efficiency arising from the starburst bis-carbazole substituted triphenylamine group.

The long-term stability of DSSCs is a critical requirement for their photovoltaic application, for which lifetime is a vital factor. A simple and efficient method has been developed to evaluate the stability of dyes by Katoh, which can accelerate the dye aging process by light irradiation on dye-loaded TiO$_2$ film without redox electrolyte.[8a-b] Grätzel and Zhu et al have also assessed the

This journal is © The Royal Society of Chemistry [year]

J. Mater. Chem. A, 2014, **[vol]**, 00–00 | **3**

photo-stability of their dyes by this method.[7f] Fig. 5a illustrates the photographs of the dye-loaded TiO$_2$ film based on **DT3** and **DW3** before and after 60 min irradiation, which displays no obvious change in the color of films. Fig. 5b-c show the absorption curves of dyes **DT3** and **DW3** after aging by light irradiation of AM 1.5 light (0, 30, and 60 min). No clear variation in absorbance was observed, suggesting they are stable enough according to Katoh's method. The excellent photo-stability of starburst **DT3** and **DW3** may be ascribed to the following contributions: (1) the bulky structure of the dyes which probably protects the TiO$_2$ surface and hinders desorption,[7c] (2) the presence of holes on the oligothiophene moieties which remarkably enhances the dye stability,[8] and (3) the carbazole donor as a photostable hole-transporting moiety for DSSCs.[7c,8c]
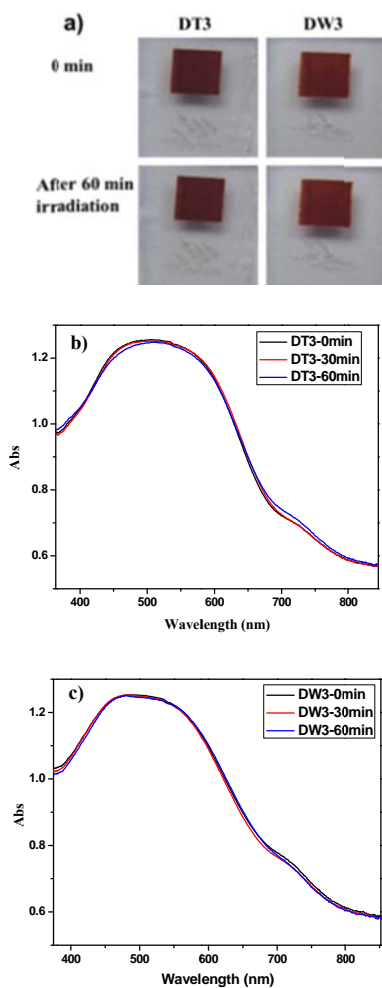

Figure 5. (a) A photograph of **DT3** and **DW3** adsorbed on 5 μm nanocrystalline TiO$_2$ films after 60 min of simulated solar light irradiation, and (b, c) absorption spectra of **DT3** and **DW3** adsorbed on nanocrystalline TiO$_2$ films before and after light irradiation for 30 and 60 min.

Conclusion

In conclusion, we have designed and synthesized two novel starburst D-D-π-π-A type dyes **DT3** and **DW3** which incorporate the following molecular engineering ideas: (1) the duplex triphenylamine and carbazole donors are alternately arranged to tune the starburst structure for better V_{oc} and overall cell performance, (2) the mixed bithiophene and EDOT units are employed to delocalize radicals for better dye stability, as well as to increase the red-shift of the absorption maximum and the molar extinction coefficients, and (3) two long alkyl chains on the bithiophene bridge are introduced to suppress the aggregation of dye molecules, enhance the solubility, and form a tightly self-assembled monolayer to block the recapture of injected electron by the I$_3^-$ or cations. The two resulting dyes exhibit excellent photo-stability as testified by the accelerating method of dye aging process by light irradiation on dye-loaded TiO$_2$ film. Strikingly, the **DT3** organic dye displays high power conversion efficiency of 10.03% in liquid DSSCs and 8.05% in QSS-DSSCs under standard global 1.5 solar conditions. To our knowledge, this is the first time such a high efficiency has been obtained for ionic liquid-based QSS-DSSCs with either pure organic or metal complex dyes as sensitizers, and also the highest efficiency observed for QSS-DSSCs based on metal-free organic sensitizers. The better conversion efficiency of **DT3**-sensitized DSSCs than **DW3** ones may arise from the red-shifted absorption, higher absorptivity above the visible spectrum, and longer electron lifetime. These findings offer a promising future for the design of starburst organic DSSCs photosensitizers and analogus derivatives by judicious molecular engineering.

EXPERIMENTAL SECTION
Materials and Reagents.

Tetrahydrofuran, toluene, and chloroform were purified using MBRAUN MB SPS-800 system. Methanol and acetonitrile were dried over molecular sieve without normal pressure distillation. Anhydrous solvents used in Suzuki coupling reaction were degassed by N$_2$ bubbling for 20 min. Optically transparent fluorine doped SnO$_2$ (FTO) conducting glass was purchased from Nippon Sheet Glass, Japan, (15 Ω/square), and cleaned by a standard procedure. All other chemicals and reagents were used as received from commercial sources without further purification. **1a-1c** and **2a-2b** were obtained as previously reported by our group.[9] The intermediates **2c-2f** and **3a** were synthesized according to the procedures in Supporting Information. The detailed synthesis of **DT3-CHO**, **DT3**, **DW3-CHO**, and **DW3** is depicted as follows.

Synthesis of DT3-CHO.

The mixture of **1c** (805 mg, 1.1 mmol), **2f** (556 mg, 0.96 mmol), Pd(PPh$_3$)$_4$ (59 mg, 0.047 mmol) was added to a Schlenk flask under nitrogen atmosphere, and then 2 M degassed anhydrous K$_2$CO$_3$ solution (359 mg, 2.6 mmol, 1.3 mL) and degassed dimethoxyethane (60 mL) were added. The reaction solution was then heated at 90 °C. After completion of the reaction as monitored by TLC, the mixture was cooled and evaporated to dryness. The residue was dissolved in ethyl acetate and the organic phase was washed with water and brine. The combined organic extracts were subsequently dried over anhydrous Na$_2$SO$_4$, filtered and evaporated to afford a crude product which was further purified by silica-gel column chromatography using petroleum ether and ethyl acetate (3:1, v/v) as eluant to obtain 772 mg yellow solid. Yield: 75%. ^{1}H-NMR (400 MHz, CDCl$_3$) δ (ppm): 9.94 (s, 1H), 8.15 (dd, J = 7.0, 5.5 Hz, 8H), 7.60 (d, J =

8.4 Hz, 2H), 7.55-7.40 (m, 8H), 7.37-7.27 (m, 8H), 7.14 (s, 1H), 7.02 (s, 1H), 6.91 (d, J = 8.5 Hz, 2H), 4.40 (dd, J = 4.7 Hz, 4H), 2.80 (m, 4H), 1.80-1.64 (m, 12H), 1.33 (s, 4H), 0.93-0.82 (m, 6H). ^{13}C-NMR (100 MHz, CDCl$_3$) δ (ppm): 179.6, 147.0, 146.3, 141.2, 141.1, 141.0, 132.6, 131.5, 129.4, 128.3, 128.2, 128.0, 128.0, 126.8, 125.9, 125.9, 125.1, 124.9, 123.5, 123.3, 123.2, 120.4, 120.3, 119.9, 119.8, 116.8, 109.8, 65.2, 64.7, 31.7, 31.7, 30.5, 30.3, 30.1, 29.7, 29.3, 29.3, 22.7, 22.6, 14.1. MALDI-TOF: m/z 1075.331 ([M$^+$]).

Synthesis of DT3.

A mixture of **DT3-CHO** (614 mg, 0.57 mmol) and cyanoacetic acid (241 mg, 2.8 mmol) was added acetonitrile (20 mL) and toluene (40 mL) under nitrogen atmosphere, and then piperidine (485 mg, 5.7 mmol) was added. The reaction solution was heated at 90 °C for 5 h. Upon cooling to room temperature, the resulting mixture was neutralized to pH 2-3 with 0.5 M aqueous HCl and extracted with ethyl acetate. The extract was washed successively with water and dried over anhydrous Na$_2$SO$_4$, filtered and evaporated to afford a crude product which was further purified by silica-gel column chromatography using dichloromethane and acetic acid (80:1, v/v) as eluant to give 522 mg dark red solid. Yield: 80%. ^{1}H-NMR (400 MHz, DMF-d_7) δ (ppm): 8.34 (s, 1H), 8.30 (d, J = 7.8 Hz, 3H), 7. 83 (d, J = 8.5 Hz, 2H), 7.72 (d, J = 8.6 Hz, 4H), 7.62-7.46 (m, 15H), 7.42 (d, J = 8.5 Hz, 2H)，7.37-7.26 (m, 4H), 4.61 (dd, J = 17.5, 4. 3 Hz, 4H), 2. 99-2.84 (m, 4H), 1.86-1.64 (m, 4H), 1.54-1.19 (m, 12H), 0.89 (t, J = 6.7 Hz, 6H); ^{13}C-NMR (100 MHz, DMF-d_7) δ (ppm): 166.0, 164.4, 149.0, 147.2, 146.6, 144.0, 142.1, 142.0, 141.1, 140.3, 138.2, 137.6, 132.7, 129.1, 128.9, 128.6, 127.1, 126.9, 126.4, 126.2, 125.7, 124.9, 123.4, 120.9, 120.7, 120.2, 117.4, 110.1, 108.0, 94.5, 66.3, 65.5, 31.73, 31.65, 30.7, 30.4, 24.4, 22.64, 22.63, 13.8. MALDI-TOF: m/z 1142.328 ([M$^+$]).

Synthesis of DW3-CHO.

3a (500 mg, 0.76 mmol), **2f** (490 mg, 0.84 mmol), copper powder (30 mg, 0.5 mmol), K$_2$CO$_3$ (520 mg, 3.8 mmol), 18-crown-6 (10 mg, 0.08mmol) was added to a flask under nitrogen atmosphere, and then 1,2-dichlorobenzene (20 mL) was added. The reaction mixture was refluxed for 18 h. The precipitate was filtered and the residue was washed with dichloromethane. The filtrate was collected and concentrated. After removal of solvent, raw product was obtained. The product was obtained by silica gel chromatography using petroleum ether and ethyl acetate (3:1, v/v) as eluant to obtain 530 mg yellow solid. Yield: 60%. ^{1}H-NMR (400 MHz, CDCl$_3$) δ (ppm): 9.98 (s, 1H), 8.64 (d, J = 9.0 Hz, 2H), 8.58 (d, J = 4.0 Hz, 1H), 7.82-7.77 (m, 2H), 7.74-7.71 (m, 5H), 7.65-7.61 (m, 4H), 7.55 (d, J = 8.8 Hz, 2H), 7.41 (s, 2H), 7.35-7.31 (m, 8H), 7.23 (s, 2H), 7.11-7.06 (m, 16H), 4.47 (dd, J = 16.0, 4.0 Hz, 4H), 2.86-2.77 (m, 4H), 1.66-1.61 (m, 4H), 1.36-1.17 (m, 12H), 0.89-0.85 (m, 6H). ^{13}C-NMR (100 MHz, CDCl$_3$) δ (ppm): 179.25, 147.24, 147.20, 146.35, 146.27, 142.90, 140.42, 140.27, 134.88, 131.73, 131.58, 129.62, 128.71, 127.80, 123.96, 123.10, 119.60, 117.17, 115.47, 112.27, 109.56, 108.13, 64.95, 64.65, 30.03, 29.39, 29.04, 28.60, 21.80, 14.01. MALDI-TOF: m/z 1168.500 ([M]$^+$).

Synthesis of DW3.

A mixture of **DW3-CHO** (117 mg, 0.10 mmol) and cyanoacetic acid (42.5 mg, 0.50 mmol) was added acetonitrile (5 mL) and chloroform (5 mL) under nitrogen atmosphere, and then piperidine (170 mg, 2.0 mmol) was added. The reaction solution was heated at 90 °C for 5 h. Upon cooling to room temperature, the resulting mixture was neutralized to pH 2-3 with 0.5 M aqueous HCl and extracted with dichloromethane. The extract was washed successively with water and dried over anhydrous Na$_2$SO$_4$, filtered and evaporated to afford a crude product which was further purified by silica-gel column chromatography using dichloromethane and acetic acid (50:1, v/v) as eluant to give 111 mg dark red solid. Yield: 91%. ^{1}H NMR (400 MHz, DMF-d_7) δ (ppm): 8.79 (s, 2H), 8.35 (s, 1H), 8.03 (s, 2H), 7.89 (d, J = 8.0 Hz, 2H), 7.85 (d, J = 8.0 Hz, 2H), 7.75 (d, J = 8. 8 Hz, 2H), 7.53 (s, 1H), 7.38 (t, J = 7.8 Hz, 8H), 7.20-7.09 (m, 16H), 4.62 (d, J = 12.0 Hz, 4H), 3.02-2.95 (m, 8H), 1.83-1.75 (m, 4H), 1.48-1.35 (m, 12H), 0.91-0.89 (m, 6H). ^{13}C NMR (400 MHz, DMF-d_7) δ (ppm): 165.1, 164.5, 148.82, 147.82, 144.71, 141.97, 140.91, 139.15, 137.58, 137.44, 136.57, 134.74, 130.67, 128.96, 128.64, 127.85, 126.63, 125.61, 125.26, 124.19, 119.78, 111.93, 111.13, 67.20, 65.94, 32.63, 32.54, 31.60, 23.45, 14.14. ESI-MS: 1220.399 ([M-H]$^-$).

Characterizations.

[1]H and ^{13}C nuclear magnetic resonance (NMR) spectroscopies were performed on a BRUKER 400 MHz with tetramethylsilane (TMS) as internal standard. Elemental analyses were carried out with an Elementar Vario EL Cube instrument. Mass spectral data were obtained on an ultrafleX-treme MALDI-TOF/TOF mass spectrometer (Bruker Daltonics). The absorption spectra of the dyes (in solution and adsorbed on TiO$_2$ films) were observed with a Shimadzu UV- 2450 spectrometer and fluorescence spectra were measured with a Hitachi F-4500 spectrometer. Cyclic voltammogram (CV) curves were obtained with a CHI 832 electrochemical analyzer using a normal three-electrode cell with dye-sensitized photoanode as working electrode, a Pt wire counter electrode, and a regular Ag/AgCl reference electrode in saturated KCl solution which was calibrated with ferrocene/ferrocenium as external reference. The supporting electrolyte was 0.1 M tetrabutylammonium hexafluorophosphate in CHCl$_3$.

Fabrication of Cells.

The anatase TiO$_2$ nanoparticles were synthesized according to our previous literature.[12] First, the Ti(OBu)$_4$ (10 mL) was added to the ethanol (20 mL) under stirring for 10 min. Then a mixture of deionized water (50 mL) and acetic acid (18 mL) was added to the solution with vigorous stirring for 1 h. The solution was moved to an autoclave and heated at 200 °C for 12 h. Finally, the precipitations were washed with deionized water and ethanol for several times, respectively. The white powder was obtained after drying in air. The as-prepared TiO$_2$ nanoparticles were anatase crystals with diameters of about 20 nm, as confirmed by SEM, TEM, and XRD. The prepared TiO$_2$ powder (1.0 g) was ground for 40 min in the mixture of acetic acid (0.2 mL), ethanol (8.0 mL), ethyl cellulose (0.5 g), and terpineol (3.0 g) to form a slurry, and then the slurry was sonicated for 5 min to obtained a viscous white TiO$_2$ paste. The TiO$_2$ paste was then screen-printed onto the surface of FTO coated glass forming photoanode film. The thickness of films can be easily controlled through repeating screen-printing times. Afterwards, a programmed heating process was carried out to remove the organic substances in the film. The as-prepared TiO$_2$ films (~15 µm) were soaked in a 0.04 M

aqueous solution of $TiCl_4$ for 30 min at 70 °C and then sintered at 520 °C for 30 min. After cooling to 80 °C, the TiO_2 electrodes were immersed into 0.3 mM optimal organic solution ($CHCl_3$/ACN/^tBuOH = 1/2/2) of the dyes and kept at room temperature for 6 h for cells with liquid electrolyte and for 12 h for cells with gel electrolyte, respectively. And then the prepared TiO_2 working electrodes were sandwiched together with Pt-counter electrode. The active area of the dye-coated TiO_2 film was 0.16 cm^2. The electrolyte was injected into the inter-electrode space. The liquid electrolyte are composed of 0.6 M 1-methyl-3-propylimidazolium iodide (PMII), 0.10 M guanidinium thiocyanate (GuNCS), 0.03 M I_2, 0.5 M *tert*-butylpyridine (t-BP) in acetonitrile and valeronitrile (85:15, v/v). For the quasi-solid state electrolyte, 12 nm silica nanoparticles (5 wt%) was mixed with 1-butyl-3-methy limidazolium iodide (BMII) based liquid electrolyte containing 0.5 M iodine (I_2) and 0.45 M benzimidazole (BI) in an agate mortar.[7c,e] The dye-adsorbed TiO_2 film as working electrode was placed on the top of a Pt coated FTO glass as counter electrode. The electrolyte was introduced into the space between two electrodes by capillary force.

Characterization of Cells.

The TiO_2 film thickness and active area of the dye-coated TiO_2 film was measured by using a profilometer (Ambios, XP-1). The current-density voltage (*J-V*) curves of the DSSCs were recorded by using a Keithley 2400 source meter under the illumination of AM 1.5 G simulated solar light. IPCEs of DSSCs were measured on the basis of a Spectral Products DK240 monochromator. Electrochemical impedance spectroscopy (EIS) was measured using an electrochemical workstation (Zahner, Zennium) with a frequency response analyzer at a bias potential of -800 mV in the dark with a frequency ranging from 10 mHz to 1 MHz. The dye-adsorbed amounts on the TiO_2 film were measured using a Shimadzu UV-2450 spectrometer.

The dye aging process.

The dye aging process experiment was operated according to the reported literatures.[7f,8a] The photostability of dyes adsorbed on the nanocrystalline films was evaluated by visible-light (>400 nm) irradiation from a solar simulator (Newport company) operating at AM 1.5 (100 mW cm^{-2}) with an ultraviolet (UV) cutoff filter. Irradiation was carried out under ambient conditions. In order to evaluate the degradation of the dyes, absorption measurements were carried out with a spectrometer (Shimadzu, UV-2450) equipped with an integrating sphere at 0, 30 and 60 min irradiation times.

Notes and references

[a] MOE Laboratory of Bioinorganic and Synthetic Chemistry, State Key Laboratory of Optoelectronic Materials and Technologies, Lehn Institute of Functional Materials, School of Chemistry and Chemical Engineering, Sun Yat-Sen University, Guangzhou 510275, China. Fax: +86-20-84115178; Tel: +86-20-84115178; Email: *liujunm@mail.sysu.edu.cn, cesscy@mail.sysu.edu.cn*
[b] *School of Computer Science and Engineering, Beihang University, Beijing 100191, China*
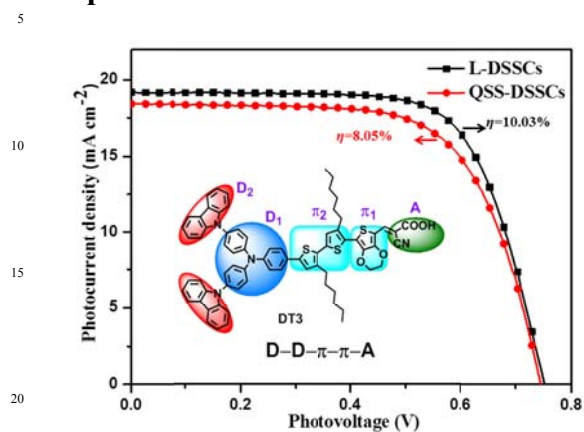[c] *State Key Laboratory of Applied Organic Chemistry, Lanzhou University, Lanzhou 730000, China*
† Electronic Supplementary Information (ESI) available: synthesis and cell fabrication. See DOI: 10.1039/b000000x/

1 B. O' Regan and M. Grätzel, *Nature*, 1991, **353**, 737-740.
2 A. Yella, H.-W. Lee, H. N. Tsao, C. Yi, A. K. Chandiran, M. K. Nazeeruddin, E. W.-G. Diau, C.-Y. Yeh, S. M Zakeeruddin and M. Grätzel, *Science*, 2011, **334**, 629-634.
3 J.-H. Yum, I. Jung, C. Baik, J. Ko, M. K. Nazeeruddin and M. Grätzel, *Energy Environ. Sci.*, 2009, **2**, 100-102.
4 W. Zeng, Y. Cao, Y. Bai, Y. Wang, Y. Shi, M. Zhang, F. Wang, C. Pan and P. Wang, *Chem. Mater.*, 2010, **22**, 1915-1925.
5 (a) Z. Ning, Y. Fu, H. Tian, *Energy Environ. Sci.*, 2010, **3**, 1170-1181; (b) A. Mishra, M. K. R. Fischer and P. Bäuerle, *Angew. Chem. Int. Ed.*, 2009, **48**, 2474-2499.
6 (a) R. F. Fink, J. Seibt, V. Engel, M. Renz, M. Kaupp, S. Lochbrunner, H.-M. Zhao, J. Pfister, F. Würthner and B. Engels, *J. Am. Chem. Soc.*, 2008, **130**, 12858-12859; (b) S. Tan, J. Zhai, H. Fang, T. Jiu, J. Ge, Y. Li, L. Jiang and D. Zhu, *Chem. Eur. J.*, 2005, **11**, 6272-6276; (c) M. C. Gather and D. D. C. Bradley, *Adv. Funct. Mater.*, 2007, **17**, 479-485.
7 (a) M. Liang and J. Chen, *Chem. Soc. Rev.*, 2013, **42**, 3453-3488; (b) Z. Ning, Q. Zhang, W. Wu, H. Pei, B. Liu and H. Tian, *J. Org. Chem.*, 2008, **73**, 3791-3797; (c) J. Tang, J. Hua, W. Wu, J. Li, Z. Jin, Y. Long and H. Tian, *Energy Environ. Sci.*, 2010, **3**, 1736-1745; (d) Z. Ning, Q. Zhang, H. Pei, J. Luan, C. Lu, Y. Cui and H. Tian, *J. Phys. Chem. C*, 2009, **113**, 10307-10313; (e) J. Tang, W. Wu, J. Hua, J. Li, X. Li and H. Tian, *Energy Environ. Sci.*, 2009, **2**, 982-990; (f) Y. Wu, M. Marszalek, S. M. Zakeeruddin, Q. Zhang, H. Tian, M. Gräzel and W. Zhu, *Energy Environ. Sci.*, 2012, **5**, 8261-8272; (g) D. P. Hagberg, J.-H. Yum, H. Lee, F. De Angelis, T. Marinado, K. M. Karlsson, R. Humphry-Baker, L. Sun, A. Hagfeldt, M. Grätzel and M. K. Nazeeruddin, *J. Am. Chem. Soc.*, 2008, **130**, 6259-6266; (h) K. R. J. Thomas, Y.-C. Hsu, J. T. Lin, K.-M. Lee, K.-C. Ho, C.-H. Lai, Y.-M. Cheng and P.-T. Chou, *Chem. Mater.*, 2008, **20**, 1830-1840; (i) W. Lee, N. Cho, J. Kwon, J. Ko and J.-I. Hong, *Chem. Asian J.*, 2012, **7**, 343-350.
8 (a) R. Katoh, A, Furube, S. Mori, M. Miyashita, K. Sunahara, N. Koumura and K. Hara, *Energy Environ. Sci.*, 2009, **2**, 542-546; (b) A. Hagfeldt, G. Boschloo, L. Sun, L. Kloo, H. Pettersson, *Chem. Rev.*, 2010, **110**, 6595-6663; (c) K. Hara, Z.-S. Wang, Y. Cui, A. Furube and N. Koumura, *Energy Environ. Sci.*, 2009, **2**, 1109-1114.
9 L.-L. Tan, H.-Y. Chen, L.-F. Hao, Y. Shen, L.-M. Xiao, J.-M. Liu, D.-B. Kuang and C.-Y. Su, *Phys. Chem. Chem. Phys.*, 2013, **15**, 11909-11917.
10 (a) P. Wang, S. M. Zakeeruddin, P. Comte, I. Exnar and M. Grätzel, *J. Am. Chem. Soc.*, 2003, **125**, 1166-1167; (b) L. Etgar, G. Schuchardt, D. Costenaro, F. Carniato, C. Bisio, S. M. Zakeeruddin, M. K. Nazeeruddin, L. Marchese and M. Graetzel, *J. Mater. Chem. A*, 2013, **1**, 10142-10147.
11 (a) R,-X. Dong, S.-Y. Shen, H.-W. Chen, C.-C. Wang, P.-T. Shih, C.-T. Liu, R. Vittal, J.-J. Lin and K.-C. Ho, *J. Mater. Chem. A*, 2013, **1**, 8471-8478; (b) C.-L. Chen, H Teng and Y.-L. Lee, *Adv. Mater.* **2011**, **23**, 4199-4204; (c) C. L. Chen, T.-W. Chang, H. Teng, C. G. Wu, C.-Y. Chen, Y.-M. Yang and Y.-L. Lee, *Phys. Chem. Chem. Phys.*, 2013, **15**, 3640-3645; (d) O. A. Ileperuma, *Mater. Technol.*, 2013, **28**, 65-70.
12 H.-Y. Chen, L. Lin, X.-Y. Yu, K.-Q. Qiu, X.-Y. Lü, D.-B. Kuang and C.-Y. Su, *Electrochim. Acta*, 2013, **92**, 117-123.

6 *J. Mater. Chem. A*, 2014, **[vol]**, 00–00

This journal is © The Royal Society of Chemistry [year]

Graphical abstract

A starburst organic sensitizer (see picture) showing extremely high overall conversion efficiency 10.03 % in liquid DSSCs and 8.05 % in quasi-solid-state DSSCs was designed. The high efficiencies are related to its wide IPCE spectrum, long electron lifetime, outstanding aggregation-resistant ability, and excellent electron injection capability from the starburst donors.